CARDIAC SURGERY

UDC 616.132-007.64

CT-fusion-guided thoracic endovascular aortic repair: Case report and literature review

A. A. Khilchuk[1,2], *A. A. Payvin*[1], *S. G. Scherbak*[2], *V. V. Guryev*[1], *E. G. Karmazanashvili*[3], *D. N. Lazakovich*[1]

[1] City Hospital no. 40,
9, ul. Borisova, Sestroretsk, St. Petersburg, 197706, Russian Federation
[2] St. Petersburg State University,
7–9, Universitetskaya nab., St. Petersburg, 199034, Russian Federation
[3] City Hospital no. 26,
2, ul. Kostyushko, St. Petersburg, 196247, Russian Federation

For citation: Khilchuk A. A., Payvin A. A., Scherbak S. G., Guryev V. V., Karmazanashvili E. G., Lazakovich D. N. CT-fusion-guided thoracic endovascular aortic repair: Case report and literature review. *Vestnik of Saint Petersburg University. Medicine*, 2021, vol. 16, issue 3, pp. 180–189.
https://doi.org/10.21638/spbu11.2021.305

Interventional and hybrid methods of treatment, combining open surgical and endovascular repairs, are the most promising areas in the surgery of the thoracoabdominal aorta. Recent studies, however, have demonstrated that complex thoracic endovascular aneurysm repair (TEVAR) is one of the most high-dose endovascular interventions. In addition, TEVAR is associated with the use of a significant volume of contrast media (CM), which can lead to contrast-induced acute kidney injury (CI-AKI). The use of advanced imaging techniques and computed tomographic fusion (CT-fusion) in routine practice can potentially reduce operation duration, radiation exposure and CM volume usage. We analyzed the literature on CT-fusion in endovascular aortic repair and present a clinical case of a 50-year-old male with a history of concomitant blunt chest trauma. CT of the chest revealed an aneurysm of the arch and descending aorta after traumatic dissection of the aorta (IIIa DeBakey, type B Stanford), post-traumatic diaphragmatic hernia of the left dome of the diaphragm with stomach and intestinal loops prolapse. The patient underwent a staged hybrid intervention — subtotal aortic arch debranching followed by CT-fusion-guided semi-arch TEVAR. CT-fusion is a dynamically developing technology, may reduce the CM volume, the duration of the procedure and radiation exposure and requires further research.

Keywords: aorta, endovascular aortic repair, aortic aneurysm, computed tomography, CT-fusion.

Introduction

Despite the rapid development of noninvasive imaging methods, thoracic aortic aneurysms and dissections remain one of the most frequent causes of sudden cardiac death, amounting to 5.9 cases per 100K people per year [1]. Aortic dissection is a violation of the integrity of its intimal and medial layers, resulting in intimal detachment and intramural hematoma. In the natural course of dissection, inflammatory response to thrombosis in the medial layer initiates further necrosis and apoptosis of aortic smooth muscle cells and elastoid degeneration, which may cause aortic aneurysm and aortic wall rupture [2]. Based on the area of proximal fenestra dissection, there are several classifications. The most common today are the DeBakey and Stanford classification systems.

According to the DeBakey classification, there are 3 types: Type I, when dissection involves the aortic arch, the ascending and descending parts of the thoracic aorta; Type II — proximal fenestration and dissection involve only the ascending aorta; Type III — proximal intimal tear is limited only to the descending thoracic aorta. Since the treatment tactics of Types I and II are similar, currently the most common anatomical classification is Stanford, according to which Type A is the proximal/ascending type, and Type B is the distal/descending one [3].

For planning various types of endovascular repair for aortic dissection, Mitchell et al. have developed a special anatomical classification based on which the aortic arch, its ascending and descending sections are divided into zones within which proximal stent-graft is fixed (Fig. 1) [4].

According to Coady et al., about 20 % of thoracic aortic aneurysms are associated with congenital connective tissue defect, the most famous of which are the Marfan, Ehlers-Danlos syndromes and some others [5]. Acquired aneurysms can be caused by aortic arterial sclerotic disease, infections (syphilitic mesaortitis, "mycotic" aneurysms), autoimmune diseases (Takayasu, Behcet's, Ormond's diseases), iatrogenic aortic lesions, and injuries, etc. [6; 7]. Traumatic aortic injury, both independently and with subsequent aneurysm formation, in the absence of diagnosis and treatment can be fatal in 80 % [7]. 75 % of thoracic aortic traumatic injuries are the result of road traffic accidents. The mechanism is based on the abrupt displacement of the heart and aortic arch relative to the fixed aortic ligament of the descending aorta [6]. Due to the lack of specific symptoms, the patient's condition is often underestimated at presentation. The optimal medical therapy of descending aortic dissection alone may lead to significant dilatation, which further requires repair. One of the risk factors of aneurysm rupture is growth rate. The average growth rate of non-traumatic thoracic aortic an-

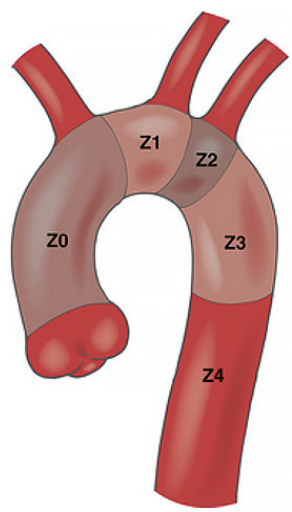

Fig. 1. Mitchell — Ishimaru graft fixation zones

Z0 — from ascending aorta to brachiocephalic trunk; Z1 — from brachiocephalic trunk to LCC artery; Z2 — from LCC artery to LSA; Z3 — from LSA to descending thoracic aorta; Z4 — to inferior thoracic aorta

Note: LCC artery — left common carotid artery; LSA — left subclavian artery.

eurysms is 0.1 cm/year, while the average growth rate of thoracic aortic aneurysms with chronic dissection is from 0.24 cm/year for small aneurysms (over 4.0 cm) to 0.48 cm/year for aneurysms over 8.0 cm in diameter [8].

Computed tomography (CT), transesophageal echocardiography and magnetic resonance imaging (MRI) are most used for the diagnosis of thoracic aortic aneurysm [9; 10]. Transthoracic echo in parasternal position enables to visualize well only the root and proximal part of the ascending aorta, so it is a low sensitive diagnostic method, in contrast to transesophageal echo, especially if the aneurysm is localized in the descending aorta [11]. CT-angiography is the fastest, noninvasive most sensitive, specific, and accessible diagnostic method providing all necessary anatomical information for planning aortic repair. CT advantages are the capability of detailed assessment of anatomy and damage type, aneurysm localization, its relationship with main branches, intimal fenestration, etc. In case of contraindications to CT-angiography, such as CM intolerance, chronic kidney disease (CKD) C3b-C4, an alternative diagnostic method is MRI. Noninvasive imaging methods allow to determine patient management tactics and preferred surgical treatment method.

The most developing and promising trend of thoracoabdominal aortic aneurysm surgery is interventional and hybrid treatment methods characterized by a combination of open surgical and endovascular aortic intervention in one procedure or two different steps. These techniques can be an alternative to standard, technically challenging open surgical interventions associated with a high risk of postoperative complications and mortality. Most authors now distinguish 3 types of hybrid interventions on aortic arch aneurysms, depending on the anatomy and presence of graft fixation zones. In case of isolated arch aneurysm, classical debranching is performed, which is basically the ligation of the aortic branch ostia and switching blood flow to the main branches on a multibranch prosthesis. Depending on proximal fenestration location, debranching can be total — when all the branches of aortic arch are switched, subtotal — when blood flow is switched along 2 or more vessels, and partial — when one vessel is switched. The second stage of intervention is single-step or delayed stent-graft implantation. Preliminary debranching allows to avoid complications in the postoperative period. According to recent publications, even with partial blocking of aortic arch branches with an endoprosthesis, the hospital risk of stroke is 8 %, while the incidence of perioperative strokes does not exceed 2 % when the brachiocephalic arteries are switched [12; 13]. In case of proximal fenestration in the ascending aorta, the 2nd type of hybrid interventions is performed — creating an adequate proximal fixation zone using the open prosthesis of the ascending aorta [14]. In extended aneurysms (mega-aortic syndrome), when both the proximal and distal graft attachment zones are missing, the 3rd type of hybrid surgery is performed — the total open repair of the ascending aorta and arch in elephant trunk modification (Borst procedure), followed by stent-graft implantation into the thoracic aorta, which is fixed with transition to the overlying prosthetic aortic part [15–17].

When performing thoracic endovascular aortic repair (TEVAR), the morphology of the proximal and distal landing zones as well as aortic size should be well examined. For the intraoperative visualization of the anatomy and orientation of the endovascular instrument, it is reasonable to use auxiliary methods of imaging. CT-fusion is a method that allows projecting a 3D-anatomical model with color markers onto a live fluoroscopic image. Data overlay aligns images with anatomical landmarks, bony or vascular, and merges

data with live fluoroscopy into a single coordinate system. The resulting CT mask automatically adapts to changes in C-arm angle, table position, and field of view. The CT mask with planning markers and lines is available throughout the operation and can be further adjusted to changing anatomy. Although the clear benefit of using CT-fusion in routine endovascular aortic repair (EVAR) and TEVAR has not yet been demonstrated, the technology allows to significantly reduce the amount of the injected CM and procedural time in advanced aortic interventions (ChEVAR, BEVAR, FEVAR) [12].

Case presentation

Patient K., 50-years-old, with a long-term course of arterial hypertension. In 2009 he was treated for the consequences of a traffic accident (a blunt thoracic and abdominal trauma). 2010 CT data show a transection in the thoracic aorta and a left hemidiaphragm defect. He has refused to undergo surgical intervention.

Upon re-examination, native CT and CT-angiography visualized posttraumatic left hemidiaphragm hernia with prolapsing large and small intestine loops, significant left lung collapse, and the postdissection aneurysm of the aortic arch and descending section of type IIIa, according to DeBakey classification, Stanford type B (Fig. 2).

The absence of an adequate proximal graft fixation zone to preserve the left common carotid (LCC) and left subclavian artery (LSA) ostia did not allow isolated TEVAR. Despite the relative safety of endograft LSA overlay, the subsequent annual risk of ischemic stroke in the posterior cerebral circulation is up to 15 % according to various authors [13]. Aggressive positioning with overlaying the left CCA mouth also significantly increases stroke risk both intra- and postoperatively. Given the relatively young age and therefore significant life expectancy, the absence of severe somatic pathology, it was decided to abandon parallel graft techniques, in-situ fenestration for LCC and LSA or for LSA, and 1 parallel LCC artery graft. Ex consilium together with cardiothoracic surgeons, it was decided to perform the subtotal 1st-stage debranching of the aortic arch followed by endovascular repair with 1 stent-graft from the Z1 zone (Figure 1).

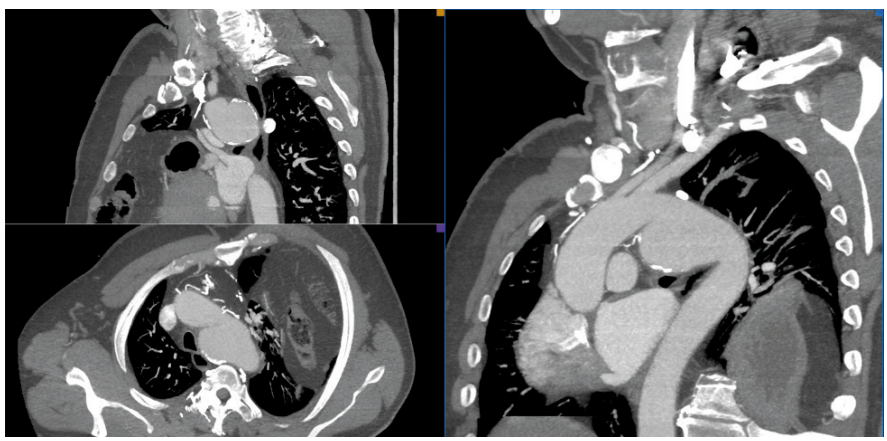

Fig. 2. Thoracic aortic aneurysm at the isthmus area (indicated by arrows), the outcome of DeBakey type IIIa traumatic dissection. The maximal diameter is 68 mm

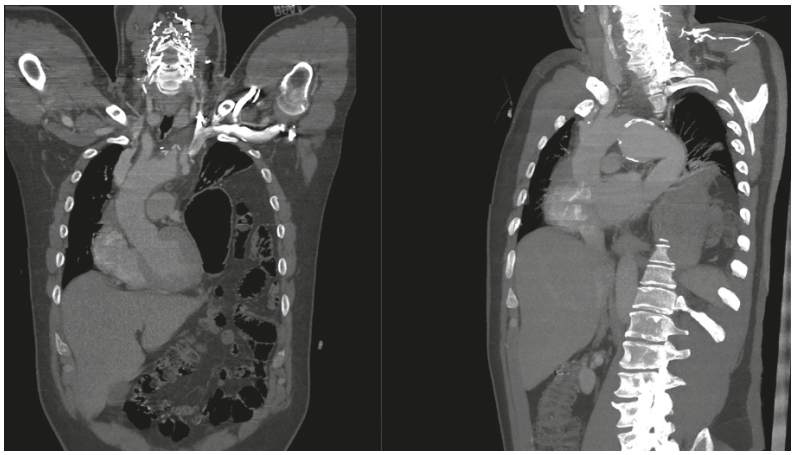

Fig. 3. Condition after subtotal LCC artery and LSA debranching. Left: arrows indicate prosthetic branches to the LCC artery and LSA. Right: arrows indicate the clipped native LCC artery and LSA with the formation of the proximal endograft fixation zone

Under the conditions of artificial blood circulation (ABC) and antegrade cerebral perfusion combined with systemic hypothermia, under cerebral oximetry control, LSA and LCC artery debranching was performed using a trifurcated arch prosthesis with an additional perfusion branch. The 1st stage was complicated by class 3a CKD (CKD-EPI GFR at 52 mL/min/1.73m^2) according to KDIGO 2012 [28]. Seven days after debranching and adequate oral and intravenous hydration, thoracic aortic CT-angiography was performed: LCC artery and LSA debranching visualized, a thoracic aortic aneurysm was visualized as an outcome of DeBakey type IIIa dissection, Stanford type B (Fig. 3). Unfortunately, the radiologists' fear of provoking contrast-induced acute kidney injury (CI-AKI) resulted in a smaller contrast medium volume and, consequently, a lower quality of CT-angiography, yet the necessary 3D information was obtained.

Eight days later, the endovascular repair of the arch and descending aorta was performed. Preoperative spiral CT-angiography data after debranching using the EVAR ASSIST software suite (GE Healthcare, France) had been previously converted into 3D-reconstruction on the Advantage Workstation VolumeShare 4.7 (GE Healthcare, France) and combined with fluoroscopy in real time (Figure 4). The entire CT mask setup was performed by the first operator intraoperatively without any additional staff. The obtained 3D-reconstruction of the thoracic aorta with color markers at brachiocephalic trunk ostium was used during the surgery as a navigation map over fluoroscopy. The right common femoral artery (CFA) was punctured under ultrasound (US) control, a 6F introducer (Terumo, Tokyo, Japan) was inserted into the arterial lumen, 2 sutures were created using Perclose ProGlide (Abbott, USA) suturing device. Additionally, through the right radial artery PigTail 5F (Cordis, USA) catheter was inserted and positioned in the ascending aorta. The right femoral artery introducer was replaced with a 12F (Boston Scientific, USA) and an ultra-hard Lunderquist (Cook Medical, USA) guidewire was inserted into the ascending aorta. An endograft Valiant Captivia VAMF3434C200TE (Medtronic, Minneapolis, USA) was positioned at Z1 zone and opened under CT-fusion control (Fig. 4).

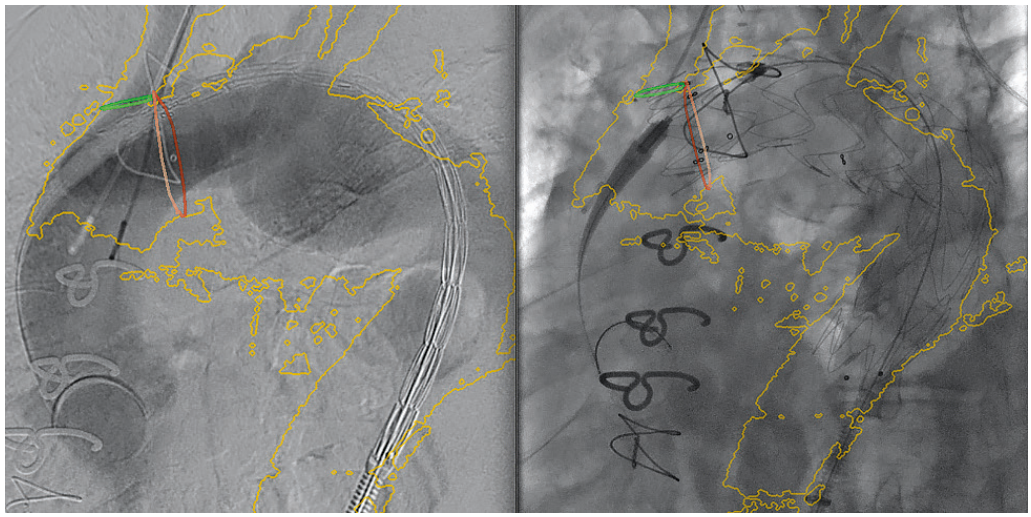

Fig. 4. Endovascular repair from Z1 zone using CT-fusion technique. Left: arrow indicates distal edge of covered endograft part, positioning by color markers of CT-model. Right: arrow indicates opened endograft in Z1 zone with coronal fixation at brachiocephalic trunk level

The control angiography showed no signs of graft malposition or visible endoleak, the aneurysm was excluded from blood flow (Fig. 5). The puncture site of the right CFA was sutured percutaneously. The operation took 45 minutes, the patient's effective dose was 3.5 mSv, the CM volume was 65 ml. The fusion of the 3D thoracic aortic model with live fluoroscopy allowed to significantly reduce the patient dose, reduce CM usage, and almost completely focus on CT-fusion during implantation.

In the early postoperative period, the patient was dynamically examined by an intensive care physician and a neurologist to control the possible early development of paraplegia. The patient's neurologic status remained unchanged after endovascular repair. Aspirin

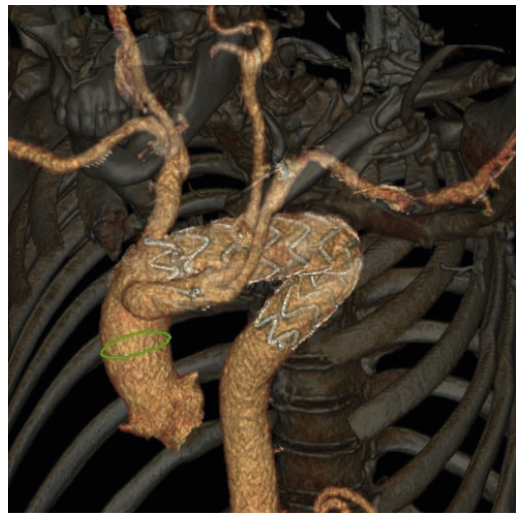

Fig. 5. Control CT-angiography after 3 months. Endograft position (indicated by arrow) from Z1 zone. Aneurysm off blood flow, no leakage and dSINE detected. LCC artery, LSA anastomoses with no signs of stenosing

Note: dSINE, distal stent-graft-induced new entry.

monotherapy was prescribed, and CT-angiography was recommended in 1 month, with monitoring serum creatinine (SCr).

After 3 months, according to CT-angiography, the aneurysm was completely excluded from the blood flow, no endoleak or new stent-induced dissections were detected. LCC artery and LSA anastomoses had no signs of stenosing. As of writing this, the patient was in good health, had no complaints, led an active lifestyle, and had been under observation for over 10 months.

Discussion

To date, the ESC guidelines for aortic disease treatment make the decision to perform TEVAR according to anatomy, pathology, comorbidities, expected life span, using multidisciplinary approach [18]. The advantage of endovascular interventions is their low injury rate and a significant reduction in patient rehabilitation periods. However, in large aneurysm interventions with fenestrations more proximal to the LSA, one-stage graft implantation is still complex or involves moderate to high surgical risks. Total or subtotal brachiocephalic arteries debranching as the first step allows to form a site for further TEVAR especially in young patients. Marullo et al., in a series of studies of patients with DeBakey type I aortic dissection who underwent ascending and aortic arch repair with debranching and subsequent endovascular treatment, showed that hospital mortality was 4.2 %, with 2-year survival rate at 92.1 ± 7.9 % [19].

Due to growing interest in hybrid therapies, high usage of CM and exposure of both patients and staff remain an important issue. Based on data from several large meta-analyses, imaging and image fusion programs during the TAE procedure have been shown to reduce both CM amount and radiation dose. Hertault et al. have demonstrated a significant decrease in CM amount injected and a trend to reduce the time of surgical intervention and fluoroscopy [20]. However, procedure time may depend on many factors, such as operator experience or perioperative complications [20]. For example, in 2011, Kobeiter et al. reported the first case of endovascular reconstruction of the thoracic aorta using an image fusion technique without CM use, meanwhile noting a sharp increase in fluoroscopy time [21]. Yet in a study by McNally et al., procedure time (from skin incision/puncture to dressing) was a major factor. According to the data presented, there was a significant reduction in radiation exposure (3.4 ± 1.9 vs. 1.38 ± 0.52 mGy; P = 0.001), fluoroscopy time (63 ± 29 vs. 41 ± 11 min; P = 0.02) and CM use (69 ± 16 vs. 26 ± 8 ml; P = 0.0002) when using intraoperative 3D-fusion CT [22].

Although the above data suggest that image fusion can reduce 2 key parameters (radiation dose and contrast volume), this technique is still relatively new. Information projected on the fluoroscopic screen is extracted from a preoperative CT scan that was performed at a different time, on a different table, and with the patient in a slightly different position. A combination of these factors can affect the accuracy of the superimposed image. In addition, accuracy may be adversely affected by anatomy distortion by endovascular devices and patient movements including breathing. Tortuous vessels can be straightened by the insertion of rigid endovascular guidewires.

Recent studies describing image fusion experience show that the CT-fusion method is not accurate enough to rely on completely [23–27]. However, despite possible inaccuracies, the image overlay technique can serve as a rough guide for the physician.

Another disadvantage of the Fusion-Imaging technology is the additional need to purchase a software suite. Moreover, the learning curve can affect fusion technique accuracy. The time taken to fuse images and fusion inaccuracies are expected to be reduced as experience increases. However, to date, there are no studies reporting any effect of the learning curve on 3D image fusion technology.

Conclusions

1. Combining 3D CT imaging with fluoroscopy is a dynamically developing technology, and to date its potential has not been fully unlocked.
2. Our clinical case and literature data suggest that the use of this technique significantly reduces CM amount injected and reduces intervention duration and fluoroscopy time.
3. The high complexity of current interventions requires the use of auxiliary techniques to combine 3D-imaging and fluoroscopy for planning and intraoperative positioning of endoprostheses. However, due to the software's complexity and high cost, this technology is still not widespread.
4. The disadvantages of this technology include the fact that the 3D model remains rigid and immobile. After all, even small changes in patient position, pronounced respiratory excursion can lead to errors in stent-graft positioning. Moreover, the anatomy of the aorta and its branches may change if rigid guidewires, catheters or endoprostheses are inserted, which requires recalibrating the 3D-model.
5. The prospect of this technique is also revealed for other interventions, such as transcatheter aortic valve replacement, atherosclerotic lesions of lower limb arteries, embolization in interventional oncology and embolization using spirals and adhesive compositions in neurosurgery.

Our center's experience has shown that the fusion of 3D images derived from CT data can facilitate intraoperative management during aortic endovascular repair, as well as significantly reduce CM amount used and reduce operation time. Drawn rings and color markers are useful for visualization, overlay correction, and manipulation control. There is a need for further development and refinement of the technique to ensure accurate, real-time automatic registration and correction of the CT mask according to the changed vascular anatomy after rigid instrument insertion.

The authors would like to express their gratitude to S. V. Vlasenko, Head of the Interventional Department, St. Petersburg State City Hospital no. 40, for his assistance in preparing this publication.

Anton A. Khilchuk provides consulting services to GE Healthcare LCC, while the other authors declare no conflicts of interest related to this publication.

References

1. Isselbacher E. M. Thoracic and abdominal aortic aneurysms. *Circulation*, 2005, vol. 111, pp. 816–28.
2. Kim Z. F., Khasanov N. R. Acute chest diseases in the recommendations of the European Society of Cardiology. *Bulletin of modern clinical medicine*, 2014, vol. 7, no. 2, pp. 85–92.
3. Podzolkov V. I., Vargina T. S. Acute aortic syndrome. *Clinical Medicine*, 2017, vol. 95, no. 9, pp. 855–861.

4. Borst H. G., Walterbusch G., Schaps D. Extensive aortic replacement using "elephant trunk" prosthesis. *Thorac. Cardiovasc. Surg.*, 1983, vol. 31, pp. 37–40.
5. Cozijnsen L., Braam R. L., Waalewijn R. What is new in dilatation of the ascending aorta? Review of current literature and practical advice for the cardiologist. *Circulation*, 2011, vol. 123, pp. 924–928.
6. Yuan S., Jing H. Cystic medial necrosis: pathological findings and clinical implications. *Rev. Bras. Cir. Cardiovasc.*, 2011, vol. 26, no. 1, pp. 107–115.
7. Belov Yu. V., Stepanenko A. B., Gens A. P., Savichev D. D. Surgical treatment of false posttraumatic aneurysm of the aortic arch with aortovenous fistula. *Angiol Sosud Khir.*, 2006, vol. 12, no. 2, pp. 127–131.
8. Detaint D., Michelena H. I., Nkomo V. T., Vahanian A., Jondeau G., Sarano M. E. Aortic dilatation patterns and rates in adults with bicuspid aortic valves: a comparative study with Marfan syndrome and degenerative aortopathy. *Heart*, 2014, vol. 100, pp. 126–134.
9. Fabian T. C., Richardson J. D., Croce M. A. Prospective study of blunt aortic injury: multicenter trial of the American Association for the Surgery of Trauma. *J. Trauma*, 1997, vol. 42, pp. 374–380.
10. Gavant M. L., Helical C. T. Grading of traumatic aortic injuries: impact on clinical guidelines for medical and surgical management. *Radiol. Clin. North. Am.*, 1999, vol. 37, pp. 553–574.
11. Ott M. C., Stewart T. C., Lawlor D. K. Management of blunt thoracic aortic injuries: endovascular stents versus open repair. *J. Trauma*, 2004, vol. 56, no. 3, pp. 565–570.
12. Quinones-Baldrich W. J., Panetta T. F., Vescera C. L. Repair of type IV thoracoabdominal aneurysm with a combined endovascular and surgical approach. *J. Vasc. Surg.*, 1999, vol. 30, no. 3, pp. 555–560.
13. Nishi H., Mitsuno M., Tanaka H. Spinal cord injury in patients undergoing total arch replacement: a cautionary note for use of the long elephant technique. *J. Thorac. Cardiovasc. Surg.*, 2011, vol. 142, pp. 1084–1089.
14. Shahverdyan R. Triple-barrel Graft as a Novel Strategy to Preserve Supra-aortic Branches in Arch-TEVAR Procedures: Clinical Study and Systematic Review. *Eur. J. Vasc. and Endovasc. Surg.*, 2013, vol. 45, no. 1, pp. 28–35.
15. Quinones-Baldrich W., Jimenez J. C., DeRubertis B., Moore W. S. Combined endovascular and surgical approach (CESA) to thoracoabdominal aortic pathology: a 10-year experience. *J. Vasc. Surg.*, 2009, vol. 49, pp. 1125–1134.
16. Patel H. J., Upchurch G. R., Eliason J. L. Hybrid debranching with endovascular repair for thoracoabdominal aneurysms: a comparison with open repair. *Ann. Thorac. Surg.*, 2010, vol. 89, pp. 1475–1481.
17. Drinkwater S. L., Goebells A., Haydar A. The incidence of spinal cord ischemia following thoracic and thoracoabdominal endovascular intervention. *Eur. J. Vasc. Endovasc. Surg.*, 2010, vol. 40, pp. 729–735.
18. Erbel R., Aboyans V., Boileau C., Bossone E., Bartolomeo R. D., Eggebrecht H., Evangelista A., Falk V., Frank H., Gaemperli O., Grabenwöger M., Haverich A., Iung B., Manolis A. J., Meijboom F., Nienaber C. A., Roffi M., Rousseau H., Sechtem U., Sirnes P. A., Allmen R. S., Vrints C. J. ESC Committee for Practice Guidelines. 2014 ESC Guidelines on the diagnosis and treatment of aortic diseases: Document covering acute and chronic aortic diseases of the thoracic and abdominal aorta of the adult. The Task Force for the Diagnosis and Treatment of Aortic Diseases of the European Society of Cardiology (ESC). *Eur. Heart J.,* 2014, vol. 35, no. 41, pp. 2873–2926.
19. Marullo A. G., Bichi S., Pennetta R. A. Hybrid aortic arch debranching with staged endovascular completion in DeBakey type I aortic dissection. *Ann. Thorac. Surg.*, 2010, vol. 90, no. 6, pp. 1847–1853.
20. Hertault A., Maurel B., Sobocinski J. Impact of hybrid rooms with image fusion on radiation exposure during endovascular aortic repair. *Eur. J. Vasc. Endovasc. Surg.*, 2014, vol. 48, pp. 382–390.
21. Kobeiter H., Nahum J., Becquemin J. P. Zero-contrast thoracic endovascular aortic repair using image fusion. *Circulation*, 2011, vol. 124, pp. 280–282.
22. McNally M. M., Scali S. T., Feezor R. J. Three-dimensional fusion computed tomography decreases radiation exposure, procedure time, and contrast use during fenestrated endovascular aortic repair. *J. Vasc. Surg.*, 2015, vol. 61, pp. 309–316.
23. Carrell TWG, Modarai B, Brown JRI, Penney GP. Feasibility and limitations of an automated 2D-3D rigid image registration 74 system for complex endovascular aortic procedures. *J. Endovasc. Ther.*, 2010, vol. 17, no. 4, pp. 527–533.
24. Fukuda T., Matsuda H., Doi S., Sugiyama M., Morita Y., Yamada M. Evaluation of automated 2D-3D image overlay system utilizing subtraction of bone marrow image for EVAR: feasibility study. *Eur. J. Vasc. Endovasc. Surg. England*, 2013, vol. 46, no. 1, pp. 75–81.
25. Schulz C. J., Schmitt M., Böckler D., Geisbüsch P. Fusion Imaging to Support Endovascular Aneurysm Repair Using 3D-3D Registration. *J. Endovasc. Ther.*, 2016, vol. 23, no. 5, pp. 791–799.

26. Schulz C. J., Schmitt M., Böckler D., Geisbüsch P. Feasibility, and accuracy of fusion imaging during thoracic endovascular aortic repair. *J. Vasc. Surg. Society for Vascular Surgery*, 2016, vol. 63, no. 2, pp. 314–322.
27. Kauffmann C., Douane F., Therasse E., Lessard S., Elkouri S., Gilbert P. Source of errors and accuracy of a two-dimensional/three-dimensional fusion road map for endovascular aneurysm repair of abdominal aortic aneurysm. *J. Vasc. Interv Radiol.*, 2015, vol. 26, no. 4, pp. 544–551.
28. Khwaja A. KDIGO clinical practice guidelines for acute kidney injury. *Nephron. Clin. Pract.*, 2012, vol. 120, no. 4, pp. 179–184.

Received: June 7, 2021
Accepted: September 28, 2021

Authors' information:

Anton A. Khilchuk — MD; anton.khilchuk@gmail.com
Artyom A. Payvin — MD, Dr. Sci., Professor; artpay@mail.ru
Sergey G. Scherbak — Dr. Sci., Professor; sgsherbak@mail.ru
Valentin V. Guryev — MD; valeant51@gmail.com
Evgeniy G. Karmazanashvili — MD; karmazan@inbox.ru
Dmitriy N. Lazakovich — MD; dim.lazakovich@yandex.ru